New Model for the Overall Transformation Kinetics of Bainite. Part 1: the Model

María Jesús Santofimia, Francisca G. Caballero, Carlos Capdevila, Carlos García-Mateo and Carlos García de Andrés.

Materalia Research Group, Department of Physical Metallurgy, Centro Nacional de Investigaciones Metalúrgicas (CENIM), Consejo Superior de Investigaciones Científicas (CSIC), Avda. Gregorio del Amo, 8. E-28040 Madrid, Spain

Synopsis

A new model for the overall transformation kinetics of bainite has been developed. Based on the displacive mechanism for the bainite transformation, the model distinguishes between the nucleation kinetics of bainitic ferrite in prior austenite grain boundaries, and at tips and adjacent positions of previously formed subunits. Some geometrical aspects of the development of the transformation have been used in the modelling. The theoretical results show that the tendencies obtained with the model are in agreement with experience.

The second part of this work deals with the experimental validation of this model.

Keywords: bainite, transformation kinetics, steels.

Abridged title: NEW MODEL for BAINITE TRANSFORMATION: MODEL

1.-Introduction

Nowadays bainitic transformation is subjected to a wide exploitation and study with the aim of improving the mechanical properties of steels. Some of the more successful applications of bainite can be found in the development of TRIP steels for automotive[1-3] and rail[4,5] industry. In all cases, the control of the microstructure formed under different thermo-mechanical treatments is fundamental for the achievement of an optimum combination of mechanical properties. In this sense, the nature of the mechanism that governs bainitic transformation is one of the more intensely discussed areas in steels. Nowadays, there are two confronted theories for the kinetic of bainite transformation, based on reconstructive and displacive mechanisms, respectively. The former theory considers[6,7] that bainite is a non-lamellar two-phase aggregate of ferrite and carbides in which the phases form consecutively, as opposed to pearlite where they form cooperatively. According to this definition, the upper limiting temperature of the bainite formation should be that of the eutectoid reaction (Ae_1), so the bainite start temperature, B_S, has no fundamental significance. Thus, the bainitic 'bay' is the highest temperature in the range where the 'coupled solute drag effect' slows down ferrite growth sufficiently so that growth can be increasingly supplemented by sympathetic nucleation, in agreement with the increasingly refined microstructure at 'sub-bay' temperatures[8,9]. The surface relief introduced during bainite growth is not clearly of an invariant-plane

strain (IPS) type for these authors, and some claim that the relieves observed are tent-shaped[10,11]. In any case, models for the development of IPS and tent-shaped surface relieves have been published for difusional phase transformations, trying to explain the surface relieves observed in bainite from a reconstructive point of view[12].

However, according to the displacive theory[13-15], the formation of bainite causes a deformation which is an IPS with a larger shear and a dilatational strain normal to the habit plane. This surface relief is considered as an evidence of a displacive mechanism of transformation. Bainite nucleation occurs by the spontaneous dissociation of specific dislocation defects which are already present in the parent phase, with the activation energy proportional to the driving force, as opposed to the inverse square relationship predicted by classical theory[16]. On the other hand, the lower C-curve in the temperature-time-transformation diagram is believed to have a characteristic flat top at a temperature T_h, which is the highest temperature at which ferrite can form by a displacive mechanism. The critical value of the maximum free energy available for paraequilibrium nucleation, ΔG_m, at the corresponding T_h temperature versus the value of T_h is a straight line. This linearity led to a function, G_N, named 'universal nucleation function' which establishes a criterion for the nucleation of bainite. The form of G_N is given by:

$$G_N = C_1 T_h - C_2 \text{ in J mol}^{-1} \qquad (1)$$

where the units of T_h are Kelvin and the values of the constants C_1 and C_2 are 3.5463 J/mol·K and 3499.4 J/mol, respectively[16]. The subunit growth is considered diffusionless and stifled by the strength of the residual austenite[17,18]. Therefore, the nucleus can only evolve into bainite plate if there is sufficient driving force available for diffusionless growth, after accounting for the store energy due to the shape deformation estimated to be[13,17] 400 J·mol^{-1}. The verification of both conditions, for nucleation and growth, will determine the value of the bainite start temperature (B_S). Soon after the growth of the subunit, the excess of carbon is partitioned into the surrounding austenite. Therefore cementite may precipitate within the carbon enriched austenite, but if steel is alloyed with enough silicon and/or aluminium, precipitation can be halted.[19]. The process continues by successive nucleation of subunits until the carbon concentration of the residual austenite reaches the value at which the free energy of bainite becomes less than that of austenite of the same composition, i.e. the T_0 curve[20-22] (or $T_0^{'}$, if the stored energy of bainite is taken into account). This trend is known as 'incomplete reaction phenomenon' because the transformation ends before the carbon concentration of austenite reaches the equilibrium value[23]. If no other reaction interacts with the process of nucleation and growth of bainite, the incomplete reaction phenomenon leads to a method for the estimation of the maximum volume fraction of bainitic ferrite, $v_{\alpha_b-\max}$, that can be formed at a given temperature. At the end of the bainitic transformation, the verification of the carbon and volume fraction balance leads to:

$$v_{\alpha_b-\max} = \frac{x_{T_0'} - \bar{x}}{x_{T_0'} - x_{\alpha_b}} \tag{2}$$

where $\bar{x}$ is the nominal carbon content of the material, $x_{T_0'}$ the carbon content of the residual austenite given by the T_0' curve and x_{α_b} the carbon content of the bainitic ferrite given by the paraequilibrium value. These assumptions have led to several kinetics models[24-29] for bainite transformation in steels that have been widely applied in research and industry as, for example, in the design of high strength bainitic steels[30,31]. Most of these models[24-28] use the Johnson, Mehl, Avrami and Kolmogorov formulation (JMAK)[32] to estimate the volume fraction of bainitic ferrite, $v_{\alpha B}$, formed in a time interval dt as follows:

$$dv_{\alpha B} = \left(1 - \frac{v_{\alpha B}}{v_{\alpha B-\max}}\right) dv_{\alpha B-ext} \tag{3}$$

where $dv_{\alpha B-ext}$ and $dv_{\alpha B}$ are the changes of the volume fraction of bainitic ferrite in dt in the extended and real volume, respectively. In these models, the time required for a bainitic ferrite sub-unit to nucleate is considered to be much greater than that for its growth, so bainite transformation is mainly controlled by the successive nucleation of subunits.

In the aforementioned models, transformation was considered to start with the nucleation of subunits at austenite grain boundaries, whereas the successive formation of subunits adjacent to the previously formed bainitic ferrite plates was taken into account through an empirical parameter named autocatalysis factor, β, having different meaning and values depending on the model. Starting with the model of Bhadeshia[24], the autocatalysis factor β indicates the increase in the number of nucleation events as transformation proceeds, in a similar way as it was used in martensite to explain the burst of transformation. Rees and Bhadeshia[25] tried to diminish arbitrariness to the autocatalysis factor and considered β as a decreasing linear function of the carbon content of the material, although the numerical results obtained were not in accordance with this assumption. In his model, Singh[27] corrected this contradiction and added simplicity to the definition of β, considering its value as an indication of the number of subunits that nucleate in a previously formed subunit, obtaining values of the order of unity. However, a clear overestimation in the contribution to the initial nucleation due only to the nucleation on subunits was found in Singh[27] model. This overestimation was solved by Opdenacker[28] applying some modifications, that were not completely justified, to the model of Singh[27]. Moreover, Matsuda and Bhadeshia[29] model completely separate the nucleation at austenite grain boundaries and on previously formed subunits. The volume fraction of bainitic ferrite formed by each sort of nucleation is thus governed by different nucleation rates. However, in the Matsuda and Bhadeshia[29] model, a new value of the autocatalysis factor, equal to 2,

is found and indicates, as in Singh[27] model, the number of subunits of bainitic ferrite nucleated on a previously formed subunit. This value of β was justified "in order to preserve the shape of the sheaf". Trying to eliminate the autocatalysis factor, Tszeng[33] used a geometrical concept of the bainite transformation, but failed in the treatment of the extended volume.

Because of the lack of an unequivocal determination of β in the models cited above, the autocatalysis factor does not seem an adequate way of considering the successive nucleation of subunits on pre-existing ones. In this work, a novel model for the kinetics of the bainite transformation is proposed. The model is based in the principles of a displacive mechanism for the bainite transformation. With the aim of eliminating the autocatalysis factor, a geometrical conception of the transformation is considered. A formulation based in simultaneous transformations is used to distinguish between kinetics of bainite nucleation at austenite grain boundaries and on previously formed subunits. The second part of this work will deal with the model experimental validation.

2.-The Model

Based on our own experimental observations, as well as those found and revised in the literature (see for example ref[34]), the authors assumed the displacive theory for bainite transformation in the

development of the kinetic model presented in this work. In order to eliminate the arbitrary autocatalysis factor, the kinetics of bainitic ferrite nucleation, both at grain boundaries and on already existing subunits, has been considered separately.

However, nucleation on subunits can take place only if there were previous nucleation events at austenite grain surfaces and, in this sense, the evolution of both *'transformation products'* is coupled. The extended volume concept of Johnson, Mehl, Avrami and Kolmogorov applied to the case of two transformation products that form simultaneously and couple[35-37] has been used during modelling.

Let $v_{\alpha_b-g}(t)$ and $v_{\alpha_b-s}(t)$ be the volume fraction of bainitic ferrite formed by nucleation at austenite grain boundaries and on subunits, respectively, after a time *t*. The maximum volume fraction of bainitic ferrite that can be formed at a given temperature, $v_{\alpha_b-\max}$, is given by the incomplete reaction phenomenon according to eq. (2). Therefore, the change in the real volume fractions of both transformation products, $dv_{\alpha_b-g}(t)$ and $dv_{\alpha_b-s}(t)$, in an interval dt are given by the change in the extended volume of both transformation products during the same dt :

$$dv_{\alpha_b-g}(t)=\left(1-\frac{v_{\alpha_b-g}(t)+v_{\alpha_b-s}(t)}{v_{\alpha_b-\max}}\right)dv_{\alpha_b-g(ext)}(t) \qquad (4)$$

$$dv_{\alpha_b-s}(t)=\left(1-\frac{v_{\alpha_b-g}(t)+v_{\alpha_b-a}(t)}{v_{\alpha_b-\max}}\right)dv_{\alpha_b-s(ext)}(t) \qquad (5)$$

where the total volume fraction of bainitic ferrite formed is given by:

$$v_{\alpha_b}(t) = v_{\alpha_b - g}(t) + v_{\alpha_b - s}(t) \tag{6}$$

Using normalised volume fractions defined as:

$$\xi_{\alpha_b - g}(t) = \frac{v_{\alpha_b - g}(t)}{v_{\alpha_b - \max}} \tag{7}$$

$$\xi_{\alpha_b - s}(t) = \frac{v_{\alpha_b - s}(t)}{v_{\alpha_b - \max}} \tag{8}$$

and substituting in eqs.(4) and (5):

$$v_{\alpha_b - \max} d\xi_{\alpha_b - g}(t) = \left(1 - \left(\xi_{\alpha_b - g}(t) + \xi_{\alpha_b - s}(t)\right)\right) dv_{\alpha_b - g(ext)}(t) \tag{9}$$

$$v_{\alpha_b - \max} d\xi_{\alpha_b - s}(t) = \left(1 - \left(\xi_{\alpha_b - g}(t) + \xi_{\alpha_b - s}(t)\right)\right) dv_{\alpha_b - s(ext)}(t) \tag{10}$$

These equations constitute a system of two coupled differential equations.

In the following, it is assumed that the transformation rate in a prior austenite grain provides the overall kinetics of bainite transformation in the material as a whole, so a volume defined by a prior austenite grain is considered. The sheaf of bainite (aggregation of ferrite plates sharing common crystallographic orientations) is considered plate shaped during transformation, following the scheme showed in Figure 1(a). The base of the sheaf in contact with the austenite grain surface is given by the volume fraction of bainitic ferrite nucleated at austenite grain boundaries. Assuming a plate shape for the subunits of bainitic ferrite, which is a reasonable assumption in medium carbon steels[38], only the subunits sides in contact with residual austenite are places susceptible of leading to a nucleation of a subunit event. A scheme of a bainitic ferrite subunit is shown in the Figure 1(b). The considered aspect ratio of the plates is the usual 0.2/10/10 microns relationship[39] The plate thickness as a function of temperature is determined accordingly to[40]:

$$u_t = 0.2 \cdot 10^{-6}\left(\frac{T-528}{150}\right) \tag{11}$$

where T is in Kelvin. The activation energy for nucleation of subunits, G^*, independently of the site of nucleation, is considered proportional to the maximum energy for nucleation ΔG_m in accordance with a mechanism of nucleation by dissociation of dislocations:

$$G^* \propto \Delta G_m \tag{12}$$

This dependence is established as:

$$G^*(t) = K_e \cdot \Delta G_m(t) + K_{2e} \tag{13}$$

where K_e and K_{2e} are two empirical constants. The application of thermodynamical models found in the literature[41-47] allows for the mathematical calculation of the maximum free energy for nucleation of bainite, ΔG_m, as a function of the chemical composition of the residual austenite along with the bainite transformation. The carbon content of the residual austenite, $x_\gamma(t)$, is estimated at every instant during transformation under the consideration that alloying elements remain at paraequilibrium. From the volume and carbon balance at any time of transformation, the value of the carbon content of the austenite, $x_\gamma(t)$ is obtained as:

$$x_\gamma(t) = \frac{\overline{x} - v_{\alpha_b}(t) x_{\alpha_b}}{1 - v_{\alpha_b}(t)} \tag{14}$$

where $v_{\alpha_b}(t)$ is the volume fraction of bainitic ferrite formed and x_{α_b} its carbon content which is given by the paraequilibrium value.

The maximum carbon content of austenite at the end of the transformation is given by the $T_0^{'}$ temperature and calculated using some thermodynamical procedures from the literature[14,46-56].

2.1 Nucleation at Austenite Grain Boundaries

Eq. (9) gives the volume fraction evolution of bainitic ferrite nucleated at austenite grain boundaries, where $dv_{\alpha_b - g(ext)}(t)$ is the differential of the extended volume fraction of bainitic ferrite formed by nucleation at austenite grain boundaries. In this context, the word 'extended' means that this phase is formed neglecting any limitation due to the fact that some of the available volume for transformation is previously occupied by bainite.

The value of $dv_{\alpha_b - g(ext)}(t)$ can be expressed as a function of the fraction of austenite grain surface occupied by bainite, $dS_{\alpha_b - g}(t)$ as:

$$dv_{\alpha_b - g(ext)}(t) = \frac{u_l \cdot dS_{\alpha_b - g}(t)}{V_\gamma} \tag{15}$$

where u_l is the length of a subunit of bainitic ferrite (see Figure 1(b)) and V_γ is the volume of an austenite grain. The lateral surface of a

bainitic ferrite plate in contact with the austenite boundary, S_u, is given by:

$$S_u = u_w \cdot u_t \tag{16}$$

where u_w and u_t are the width and thickness of a subunit. The number of subunits nucleated at austenite grain boundaries in dt is given by $I_{\alpha_b - g} \cdot S_\gamma \cdot dt$, where $I_{\alpha_b - g}$ is the nucleation rate per surface of austenite grain and S_γ the lateral surface of an austenite grain. Therefore, it is possible to calculate the lateral surface of an austenite grain occupied by bainite in a dt as:

$$dS_{\alpha_b - g(ext)}(t) = S_u \cdot I_{\alpha_b - g}(t) S_\gamma \cdot dt \tag{17}$$

It is important to point out that this calculation does not take into account that the available surface for bainite nucleation decreases with the progress of the nucleation at austenite grain boundaries, neither that this nucleation is limited to an austenite grain. This is the reason why this is a calculation of the extended surface of austenite occupied by bainite, $dS_{\alpha_b - g(ext)}(t)$. Using Cahn's formulation of the extended surface[57] a new differential equation is obtained:

$$dS_{\alpha_b-g}(t)=\left(1-\frac{S_{\alpha_b-g}(t)}{S_{\alpha_b-\max}}\right)S_u\cdot I_{\alpha_b-g}(t)\cdot S_\gamma\cdot dt \tag{18}$$

The value of $S_{\alpha_b-\max}$ is an estimation of the maximum surface of austenite grain that can be occupied by bainite. The main limitation of this surface is the value of the austenite grain surface, S_γ.

$$S_{\alpha_b-\max}\le S_\gamma \tag{19}$$

However, the maximum volume fraction of bainitic ferrite that can be formed at every temperature, $v_{\alpha_b-\max}$, is limited according to the incomplete reaction phenomenon and can be determined for a given chemical composition and transformation temperature. The maximum volume fraction of bainitic ferrite that can be formed in an austenite grain, $V_{\alpha_b-\max(1\gamma)}$, is calculated as:

$$V_{\alpha_b-\max(1\gamma)}=v_{\alpha_b-\max}\cdot V_\gamma \tag{20}$$

Assuming that this amount of bainitic ferrite is nucleated at austenite grain boundaries:

$$V_{\alpha_b-\max(1\gamma)} = S_{\alpha_b-\max} \cdot u_a \tag{21}$$

From eqs. (20) and (21) a new limitation for $S_{\alpha_b-\max}$ is found:

$$S_{\alpha_b-\max} \leq \frac{v_{\alpha_b-\max} V_\gamma}{u_a} \tag{22}$$

A reasonable estimation of $S_{\alpha_b-\max}$ can be obtained from the most restrictive of the conditions given by eqs. (19) and (22).

Finally, substituting eqs. (15) and (17) in eq. (9):

$$v_{\alpha_b-\max} d\xi_{\alpha B-g}(t) = \left[1-\left(\xi_{\alpha_b-g}(t)+\xi_{\alpha_b-s}(t)\right)\right]\frac{u_l}{V_\gamma}\left(1-\frac{S_{\alpha_b-g}(t)}{S_{\alpha_b-\max}}\right) S_u \cdot I_{\alpha_b-g}(t) \cdot S_\gamma \cdot dt \tag{23}$$

since:

$$u = u_l \cdot S_u \tag{24}$$

and

$$S_V = \frac{S_\gamma}{V_\gamma} \tag{25}$$

the differential equation changes to:

$$d\xi_{\alpha_b - g}(t) = \frac{u \cdot I_{\alpha_b - g}(t) \cdot S_V}{v_{\alpha_b - \max}} \left[1 - \left(\xi_{\alpha_b - g}(t) + \xi_{\alpha_b - s}(t)\right)\right] \left(1 - \frac{S_{\alpha_b - g}(t)}{S_{\alpha_b - \max}}\right) \cdot dt \tag{26}$$

Time evolution of bainite nucleated at austenite grain boundaries is given by eqs. (18) and (26).

On the other hand, the general form of $I_{\alpha_b - g}$, defined as the nucleation rate per unit of surface of austenite grain, is:

$$I_{\alpha_b - g}(t) = N_{\alpha_b - g}(t) \cdot \nu \cdot \exp\left[-\frac{G^*(t)}{RT}\right] \tag{27}$$

where ν is a frequency, G^* is the activation energy for nucleation of subunits and $N_{\alpha_b - g}$ is the number of bainite nuclei per unit of austenite surface in the instant of calculation. The number of nuclei at austenite grain boundaries decreases with the diminution of the austenite surface

available for nucleation. Evaluating the value of N_{α_b-g} in an austenite grain and taking into account that the maximum surface available for transformation is $S_{\alpha_b-\max}$ yields:

$$N_{\alpha_b-g}(t) \propto \frac{S_{\alpha_b-\max} - S_{\alpha_b-g}(t)}{S_\gamma} \tag{28}$$

An estimation of N_{α_b-g} could be obtained dividing the available surface for transformation between the width of a subunit in contact with the austenite grain surface that fit in the available surface and between the surface of the whole austenite grain. Including an empirical constant, K_{Ng}:

$$N_{\alpha_b-g} = K_{Ng} \frac{\left(S_{\alpha_b-\max} - S_{\alpha_b-g}(t)\right) / S_u}{S_\gamma} \tag{29}$$

Eq. (29) is consistent with the fact that when S_{α_b-g} reaches its maximum value given by $S_{\alpha_b-\max}$, then N_{α_b-g} reaches the zero.

2.2 Nucleation on Previously Formed Subunits

The term $dv_{\alpha_b-s(ext)}$ in eq. (10) can be calculated as the number of bainitic ferrite subunits nucleated on previously formed subunits inside

an austenite grain in a time dt multiplied by the volume u of each subunit:

$$dv_{\alpha_b - s(ext)}(t) = u \cdot I_{\alpha_b - s}(t) \cdot dt \tag{30}$$

where $I_{\alpha_b - s}(t) \cdot dt$ gives the number of subunits created in a dt. $I_{\alpha_b - s}$ is the number of subunits that are nucleated on subunit in an austenite grain per unit of volume and time. Substituting in eq. (10):

$$d\xi_{\alpha_b - s}(t) = \frac{u \cdot I_{\alpha_b - s}(t)}{v_{\alpha_b - \max}} \left(1 - \left(\xi_{\alpha_b - g}(t) + \xi_{\alpha_b - s}(t)\right)\right) dt \tag{31}$$

which is the third differential equation to solve along with eqs. (18) and (26) to obtain the temporal evolution of the volume fraction of bainitic ferrite.

The general form of $I_{\alpha_b - s}$ is:

$$I_{\alpha_b - s}(t) = N_{\alpha_b - s}(t) \cdot \nu \cdot \exp\left[-\frac{G^*(t)}{RT}\right] \tag{32}$$

As in the case of nucleation at austenite grain boundaries, ν is a frequency, G^* is the activation energy for nucleation of subunits and $N_{\alpha_b - s}(t)$ is the number of nuclei per volume unit for nucleation on subunit in a certain time of transformation. Since the subunits nucleated on bainite are assumed to be accumulated at the tip or lateral plates of the previously formed subunits, the number of nucleation sites on subunit is considered proportional to the number of sides of subunits in contact with the residual austenite. All the subunits of bainitic ferrite nucleated at austenite grain boundaries are assumed to be piled in the base of only one sheaf plate shaped occupying a surface given by $S_{\alpha_b - g}(t)$. Assuming a square shaped base:

$$p_w(t) = p_t(t) \tag{33}$$

then, at any time it is verified that:

$$S_{\alpha_b - g}(t) = p_w(t) \cdot p_t(t) = p_w^2(t) \tag{34}$$

The dimensions of the sheaf should verify that the volume of bainitic ferrite formed in an austenite grain after a time t, $V_{\alpha_b}(t)$, is equal to the surface of austenite grain occupied by bainite, $S_{\alpha_b - g}$, multiplied by the height of the sheaf:

$$V_{\alpha_b}(t) = p_l(t) \cdot S_{\alpha_b - g}(t) \tag{35}$$

From this relationship, the time evolution of the sheaf height can be obtained. The volume of the sheaf of bainite can be determined from the normalised volume fraction of bainitic ferrite, the maximum volume fraction of bainitic ferrite that can be formed at a temperature according to the incomplete reaction phenomenon and the volume of an austenite grain as follows:

$$V_{\alpha_b}(t) = \xi_{\alpha_b}(t) \cdot v_{\alpha_b - \max} \cdot V_\gamma \tag{36}$$

Thus, the three dimensions of the considered sheaf at any instant of time can be determined from eqs. (34)-(36). The number of sides of subunits in contact with the residual austenite at any time of transformation, $n_u(t)$, can be estimated from the geometrical considerations explained above and the dimensions of the sheaf. Therefore, the number of subunits per volume unit of austenite, including an empirical constant, K_{Ns}, is given by:

$$N_{\alpha_b - s}(t) = K_{Ns} \frac{n_u(t)}{V_\gamma} \tag{37}$$

3.-Analysis of the Predictions of the Model

The presented model has been programmed using FORTRAN90 code. The chemical composition of the steel, the austenite grain size and the temperature of the isothermal treatment are the inputs of the program. Calculation of the T_0 and T_0' curves, along with the successive calculation of $\Delta G_m(t)$ are limited to the interval of chemical compositions showed in Table 1[58]. The system of differential equations is solved by the Runge-Kutta method of fourth order. Table 2 shows the values of the used parameters in the execution of the programme.

The behaviour of the model has been tested by means of the prediction of the experimentally well-known effect that carbon, manganese and cobalt have in the bainite transformation. Manganese is known for its ability to slow down the bainite transformation and to decrease the maximum carbon content of the austenite at the end of the transformation[30,31]. On the other hand, recent investigations have shown that cobalt exerts the opposite effect[59]. Table 3 shows the chemical compositions used for this theoretical analysis along with the values of the bainite and martensite start temperatures (B_S and M_S, respectively) calculated following the thermodynamical model of

Bhadeshia[45,58]. A prior austenite grain size of 40 μm has been assumed for the kinetics calculations.

The effect of carbon on the kinetics of bainite formation at 500ºC is shown in Figure 2. The nominal carbon content of the material determines the value of x_γ at the beginning of the transformation, as can be observed from Figure 2(a). However, at the end of the transformation, the value of x_γ reaches the same value in the three alloys. This is in accordance with the incomplete reaction phenomenon because, following this theory, the original carbon content of the material does not affect the T_0' curve of an alloy. As a consequence, the chemical composition of the residual austenite of the three alloys is the same at the end of the bainitic transformation. This is the reason why the value of ΔG_m, which depends on the chemical composition of the material, tends to the same value in the three alloys (Figure 2(b)). A lower value of ΔG_m is obtained in the alloy with lower carbon content, which is the alloy Fe-0.2C and, therefore, the kinetics of the bainitic transformation during the initial instants of transformation is more rapid in this alloy. However, the alloy Fe-0.5C possesses the highest nominal carbon content of the considered alloys, i.e., a value which is the nearest to the final carbon content given by $x_{T_0'}$. Therefore, the austenite carbon content of the alloy Fe-0.5C reaches its final value in a shorter time than the other alloys, which confers certain kinetic advantage in the progress of the transformation to this alloy. These differences have not affected the time spent to reach the end of the bainitic transformation, which is approximately the same in all the cases (Figure 2(c)). Finally, as was expected, the maximum volume

fraction of bainitic ferrite that can be achieved in each alloy increases as the alloy carbon content decreases, in accordance with the incomplete reaction phenomenon (Figure 2(d)).

The predictions corresponding to an isothermal transformation at 450ºC for the alloys Fe-0.3C, Fe-0.3C-1Mn and Fe-0.3C-2Mn are presented in Figure 3. Figure 3(b) shows that as the manganese content is lowered, the smaller are the obtained initial and final ΔG_m values, which lead to a faster transformation kinetics (Figure 3(d)). The values of x_γ obtained at the end of the transformation (Figure 3(a)), suggest that the addition of manganese shifts the $T_0^{'}$ curve to lower carbon contents of the residual austenite at the end of the transformation, in other words a lower value of the maximum volume fraction of bainitic ferrite, as shown in Figure 3(c). Likewise, the displacement of the $T_0^{'}$ curve to lower values of the carbon content with the addition of manganese leads to the fact of that the residual austenite with more manganese possesses carbon content closer to the value expected at the end of the transformation. This aspect of the model agrees with the small variation of ΔG_m predicted along the transformation in the alloy with more manganese (Figure 3(b)), since its corresponding residual austenite changes the chemical composition to a lower extent than the other alloys studied.

Specifically, Figure 4 shows the results corresponding to the volume fraction of bainitic ferrite isothermically formed at 500ºC. In opposition to the observed effects of manganese, cobalt leads to a decrease of the value of ΔG_m and an increase in x_γ, i.e., a

displacement of the $T_0^{'}$ curve to higher carbon content. Consequently, cobalt leads to an acceleration of the bainitic transformation and to a higher value of the maximum volume fraction of bainitic ferrite formed at the end of the transformation. The predicted effect of the cobalt obtained with the model is also in agreement with experimental studies[59].

4.-Conclusion

A model for the kinetics of the bainite transformation has been proposed. The model is based on the principles of a displacive mechanism for the bainite transformation. A geometrical conception of the transformation has led to the elimination of the autocatalysis factor. The separation between the kinetics of nucleation both at austenite grain boundaries and on previously formed subunits has been carried out by a coupled equations formulation. The theoretical study of the results shows that the tendencies obtained with the model are in good agreement with experience.

5.-Acknoledgement

The authors acknowledge financial support from the European Coal and Steel Community (ECSC agreement number 7210-PR/345) and the Spanish Ministerio de Ciencia y Tecnología (Project-MAT 2002-10812 E). C. Garcia-Mateo would like to thank Spanish Ministerio de Ciencia y Tecnología for the financial support in the form of a Ramón y Cajal contract (RyC 2004 Program). All the authors would also like to express their gratitude to H. K. D. H. Bhadeshia for fruitful discussions.

6. References

1) P. J. Jacques: Curr. Opin. Solid State Mater. Sci. **8** (2004) 259-265.

2) B. C. De Cooman: Curr. Opin. Solid State Mater. Sci. **8** (2004) 285-303.

3) P. Jacques, E. Girault, T. Catlin, N. Geerlofs, T. Kop, S. van der Zwaag and F. Delannay: Mater. Sci. Eng. A **273-275** (1999) 475-479.

4) H. A. Aglan, Z. Y. Liu, M. F. Hassan, M. Fateh: J. Mater. Proc.Technol. **151** (2004) 268-274.

5) K. Sawley and J. Kristan: Fatigue Fract. Eng. Mater. Struct. **26** (2003) 1019-1029.

6) H. I. Aaronson: *The Decomposition of Austenite by Diffusional Processes*, ed. V. F . Zackary and H. I. Aaronson (Interscience Publishers, New York, 1962) pp. 387-546.

7) H. I. Aaronson: *The Mechanism of Phase Transformations in Crystalline Solids,* (The Institute of Metals, London, 1969) pp. 270-281.

8) H. I. Aaronson, G. Spanos and W. T. Reynolds Jr: Scr. Mater. **47** (2002) 139-144.

9) W. T. Reynolds Jr., F. Z. Li., C. K. Shui and H. I. Aaronson: Metall. Trans. A 21 (1990) 1433-1463.

10) H. S. Fang, X. Z. Bo and J. J. Wang: Mater. Trans. **39** (1998) 1463-1470.

11) H. I. Aaronson, J. M. Rigsbee, B. C. Muddle and J. F. Nie: Scr. Mater. **47** (2002) 207-212.

12) J. P. Hirth, G. Spanos, M. G. Hall and H. I. Aaronson: Acta Mater. **46** (1998) 857-868.

13) H. K. D. H. Bhadeshia: Acta Metall. **29** (1981) 1117-1130.

14) H. K. D. H. Bhadeshia and D. V. Edmonds: Acta Metall. **28** (1980) 1265-1273.

15) H. K. D. H. Bhadeshia: Scr. Metall. **14** (1980) 821-824.

16) C. Garcia-Mateo and H. K. D. H. Bhadeshia: Mater. Sci. Eng. A **378** (2004) 289-292.

17) H. K. D. H. Bhadeshia and J. W. Christian: Metall. Trans. A **21** (1990) 767-797.

18) S. B. Singh and H. K. D. H. Bhadeshia: Mater. Sci. Eng. A **12** (1996) 610-612.

19) H. K. D. H. Bhadeshia and D. V. Edmonds: Metall. Trans. A **10** (1979) 895-907.

20) H. K. D. H. Bhadeshia and A. R. Waugh: Acta Metall. **30** (1982) 775-784.

21) L. C. Chang and H. K. D. H. Bhadeshia: Mater. Sci. Eng. A **184** (1994) L17-L20.

22) I. Stark, G. D. Smith and H. K. D. H. Bhadeshia: *Solid-Solid Phase Transformations*, ed. by G. W. Lorimer (Institute of Metals, London, 1988) pp. 211-215.

23) H. K. D. H. Bhadeshia: *Proc. of the Int. Solid-Solid Phase Transformations Conference*, (The Metall. Soc. of the A.I.M.E., Pittsburgh, 1981) pp. 1041-1048.

24) H. K. D. H. Bhadeshia: Journal de Physique IV France **43** (1982) Colloque C4, 443-448.

25) G. I. Rees and H. K. D. H. Bhadeshia: Mater. Sci. Technol. **8** (1992) 985-993.

26) N. A. Chester and H. K.D. H. Bhadeshia: Journal de Physique IV France **7** (1997) Colloque C5, 41-46.

27) S. B. Singh: *Phase Transformations from Deformed Austenite*, Ph.D. Thesis, (University of Cambridge, Cambridge, UK, 1998).

28) P. Opdenacker: *The Rate of the Bainite Transformation*, Ph.D. Thesis, (University of Cambridge, Cambridge, UK, 2001).

29) H. Matsuda and H. K. D. H. Bhadeshia: Proc. R. Soc. London A **460** (2004) 1707-1722.

30) F. G. Caballero, H. K. D. H. Bhadeshia, K. J. A. Mawella, D. G. Jones and P. Brown: Mater. Sci. Technol. **17** (2001) 512-516.

31) F. G. Caballero, H. K. D. H. Bhadeshia, K. J. A. Mawella, D. G. Jones and P. Brown: Mater. Sci. Technol. **17** (2001) 517-522.

32) J. W. Christian: *Theory of Transformations in Metals and Alloys,* Part 1, 2nd. ed., (Pergamon Press, Oxford, UK, 1975) pp. 15-20.

33) T. C. Tszeng: Mater. Sci. Eng. A **293** (2000) 185-190.

34) H. K. D. H. Bhadeshia: *Bainite in Steels*, 2nd Ed. (The Institute of Materials, London, UK, 2001) pp. 19-61.

35) S. J. Jones and H. K. D. H. Bhadeshia: Acta Mater. **45** (1997) 2911-2920.

36) T. Kasuya, K. Ichikawa, M. Fuji and H. K. D. H. Bhadeshia: Mater. Sci. Technol. **15** (1999) 471-473

37) H. K. D. H. Bhadeshia: *Proceedings of Solid-Solid Phase Transformations Conference,* eds M. Koiwa, K. Otsuka and T. Miyazaki (Japan Institute for Metals, Kyoto, Japan, 1999) pp. 1445-1452.

38) H. K. D. H. Bhadeshia: *Bainite in Steels*, 2nd Ed. (The Institute of Materials, London, UK, 2001) pp. 21-22.

39) R. W. K. Honeycombe, H. K. D. H. Bhadeshia: *Steels. Microstructure and Properties*. (2nd. ed., Butterworth-Heinemann, Oxford, UK, 2000) pp. 115-119.

40) S. V. Parker: *Modelling of Phase Transformations in Hot-Rolled Steels*, PhD. Thesis, (University of Cambridge, Cambridge, UK, 1997)

41) H. K. D. H. Bhadeshia: *Bainite in Steels*, 2nd Ed. (The Institute of Materials, London, UK, 2001) pp. 130-131.

42) J. R. Lacher: Proc. Cambridge Philos. Soc. **33** (1937) 518-523.

43) R. H. Fowler and E. A. Guggenhiem: *Statistical Thermodynamics* (Cambridge University Press, New York, 1939) pp. 442

44) H. I. Aaronson, H. A. Domian and G. M. Pound: Trans. Metal. Soc. AIME **236** (1966) 753-767.

45) H. K. D. H. Bhadeshia: Metal Sci. **16** (1982) 159-165.

46) L. Kaufman, E. V. Clougherty and R. J. Weiss: Acta Metall. **11** (1963) 323-335.

47) H. K. D. H. Bhadeshia: Materials Algorithms Project, http://www.msm.cam.ac.uk/map/mapmain

48) H. K. D. H. Bhadeshia: Metal Sci. **14** (1980) 230-232.

49) G. J. Shiflet, J. R. Bradley and H. I. Aaronson: Metall. Trans. **9** (1978) 999-1008.

50) H. K. D. H. Bhadeshia: Metal Sci**. 15** (1981) 178-180.

51) B. Uhrenius: Scand. J. Metall**. 2** (1973) 177

52) C. Zener: Trans. AIME **167** (1946) 550-595.

53) J. C. Fisher: Metall. Trans. **185** (1949) 688-690.

54) C. Zener: Trans. AIME **203** (1955) 619-630.

55) H. Johansson: Archiv für Eisenhuttenwesen **11** (1937) 241.

56) H. I. Aaronson, H. A. Domian and G. M. Pound: Trans. Metall. Soc. AIME **236** (1966) 768-780.

57) J. W. Cahn: Acta Metall. **4** (1956) 449-459.

58) H. K. D. H. Bhadeshia: Materials Algorithms Project, http://www.msm.cam.ac.uk/map/steel/programs/mucg73-b.html.

59) C. García-Mateo, F. G. Caballero and H. K. D. H. Bhadeshia: ISIJ Int. **43** (2003) 1821-1825.

Number of letters and words

Letters: 30426

Words: 4867

List of captions of Tables and Figures

Table 1 Interval of limitation of the chemical compositions in the calculation of $\Delta G_m(t)$ and the T_0 and T_0' curves in the program.

Table 2 Numerical values of the empirical constants of the model.

Table 3 Chemical composition and predictions of B_S and M_S of the theoretical alloys chose for studying the tendencies of the model.

Figure 1 Scheme of (a) the bainite sheaf and (b) a subunit of plate shaped bainitic ferrite.

Figure 2 Predicted values of (a) x_γ, (b) ΔG_m, (c) ξ_b and (d) v_b for the steels Fe-0.2C, Fe-0.3C and Fe-0.5C of Table 3 considering an isothermal transformation at 500ºC.

Figure 3 Predicted values of (a) x_γ, (b) ΔG_m, (c) ξ_b and (d) v_b for the steels Fe-0.3C, Fe-0.3C-1Mn and Fe-0.3C-2Mn of Table 3 considering an isothermal transformation at 450ºC.

Figure 4 Predicted values of (a) x_γ, (b) ΔG_m, (c) ξ_b and (d) v_b for the steels Fe-0.3C, Fe-0.3C-1Co and Fe-0.3C-2Co of Table 3 considering an isothermal transformation at 500ºC.

Tables and Figures

Table 1 Interval of limitation of chemical compositions in the calculation of $\Delta G_m(t)$, T_0 and $T_0^{'}$ curves in the program.

Element	C	Si	Mn	Ni	Mo	Cr	V	Co	Cu	Al	W
Minimum (mass %)	0.001	0.000	0.000	0.000	0.000	0.000	0.000	0.000	0.000	0.000	0.000
Maximum (mass %)	2.0	2.5	3.5	3.5	3.5	3.5	3.5	1.5	4.0	2.0	2.0

Table 2 Numerical values of the empirical constants of the model.

Empirical constant	*Value*
K_{Ng}	$1.0 \cdot 10^{-10}$
K_{Ns}	$2.0 \cdot 10^{-10}$
K_e	38
K_{2e} / J·mol^{-1}	130000

Table 3 Chemical composition and predictions of B_S and M_S of the theoretical alloys chose for studying the tendencies of the model.

Steel	B_S / ºC	M_S / ºC
Fe-0.2C	625	480
Fe-0.3C	585	435
Fe-0.5C	525	355
Fe-0.3C-1Mn	540	390
Fe-0.3C-2Mn	495	345
Fe-0.3C-1Co	540	390
Fe-0.3C-2Co	495	345

Figures

Figure 1 Scheme of (a) the bainite sheaf and (b) a subunit of plate shaped bainitic ferrite.

Figure 2 Predicted values of (a) x_γ, (b) ΔG_m, (c) ξ_b and (d) v_b for the steels Fe-0.2C, Fe-0.3C and Fe-0.5C of Table 3 considering an isothermal transformation at 500ºC.

Figure 3 Predicted values of (a) x_γ, (b) ΔG_m, (c) ξ_b and (d) v_b for the steels Fe-0.3C, Fe-0.3C-1Mn and Fe-0.3C-2Mn of Table 3 considering an isothermal transformation at 450ºC.

Figure 4 Predicted values of (a) x_γ, (b) ΔG_m, (c) ξ_b and (d) v_b for the steels Fe-0.3C, Fe-0.3C-1Co and Fe-0.3C-2Co of Table 3 considering an isothermal transformation at 500ºC.

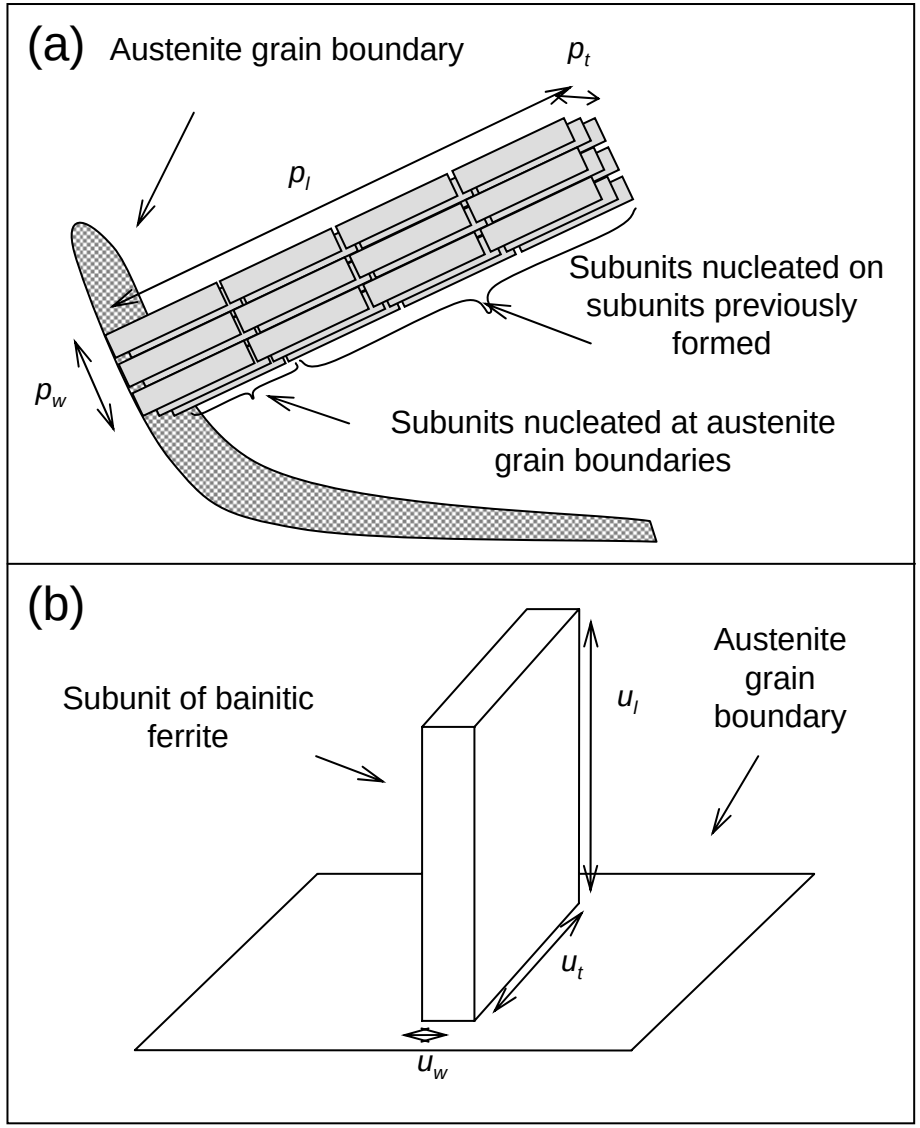
(a)
Austenite grain boundary
p_t
p_l
Subunits nucleated on subunits previously formed
p_w
Subunits nucleated at austenite grain boundaries
(b)
Subunit of bainitic ferrite
u_l
Austenite grain boundary
u_t
u_w

Figure 1

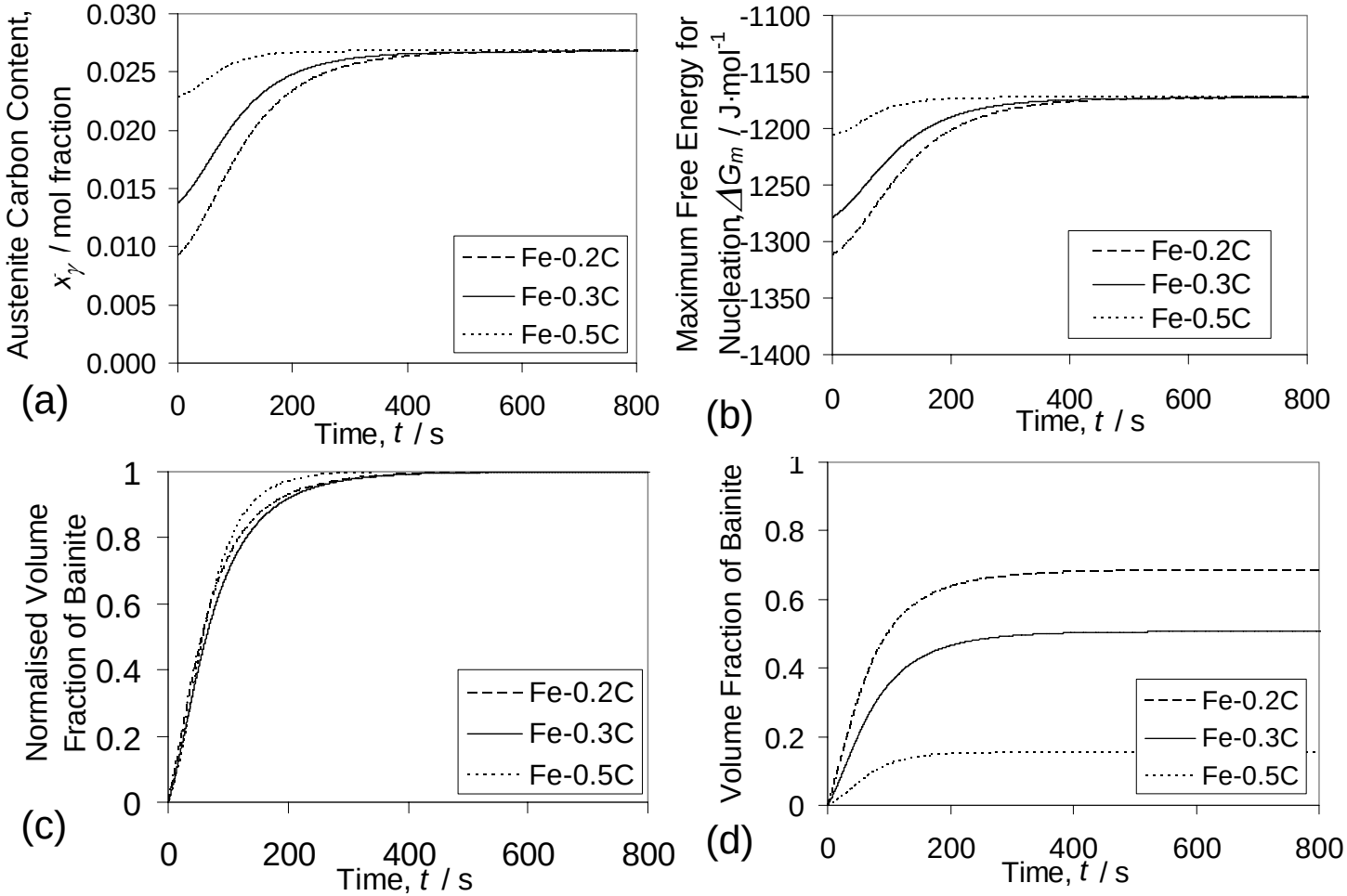
Austenite Carbon Content, x_γ / mol fraction
0.030
0.025
0.020
0.015
0.010
0.005
0.000
Fe-0.2C
Fe-0.3C
Fe-0.5C
(a)
0
200
400
600
800
Time, t / s
Maximum Free Energy for Nucleation, ΔG_m / J·mol^{-1}
-1100
-1150
-1200
-1250
-1300
-1350
-1400
Fe-0.2C
Fe-0.3C
Fe-0.5C
(b)
0
200
400
600
800
Time, t / s
Normalised Volume Fraction of Bainite
1
0.8
0.6
0.4
0.2
0
Fe-0.2C
Fe-0.3C
Fe-0.5C
(c)
0
200
400
600
800
Time, t / s
Volume Fraction of Bainite
1
0.8
0.6
0.4
0.2
0
Fe-0.2C
Fe-0.3C
Fe-0.5C
(d)
0
200
400
600
800
Time, t / s

Figure 2

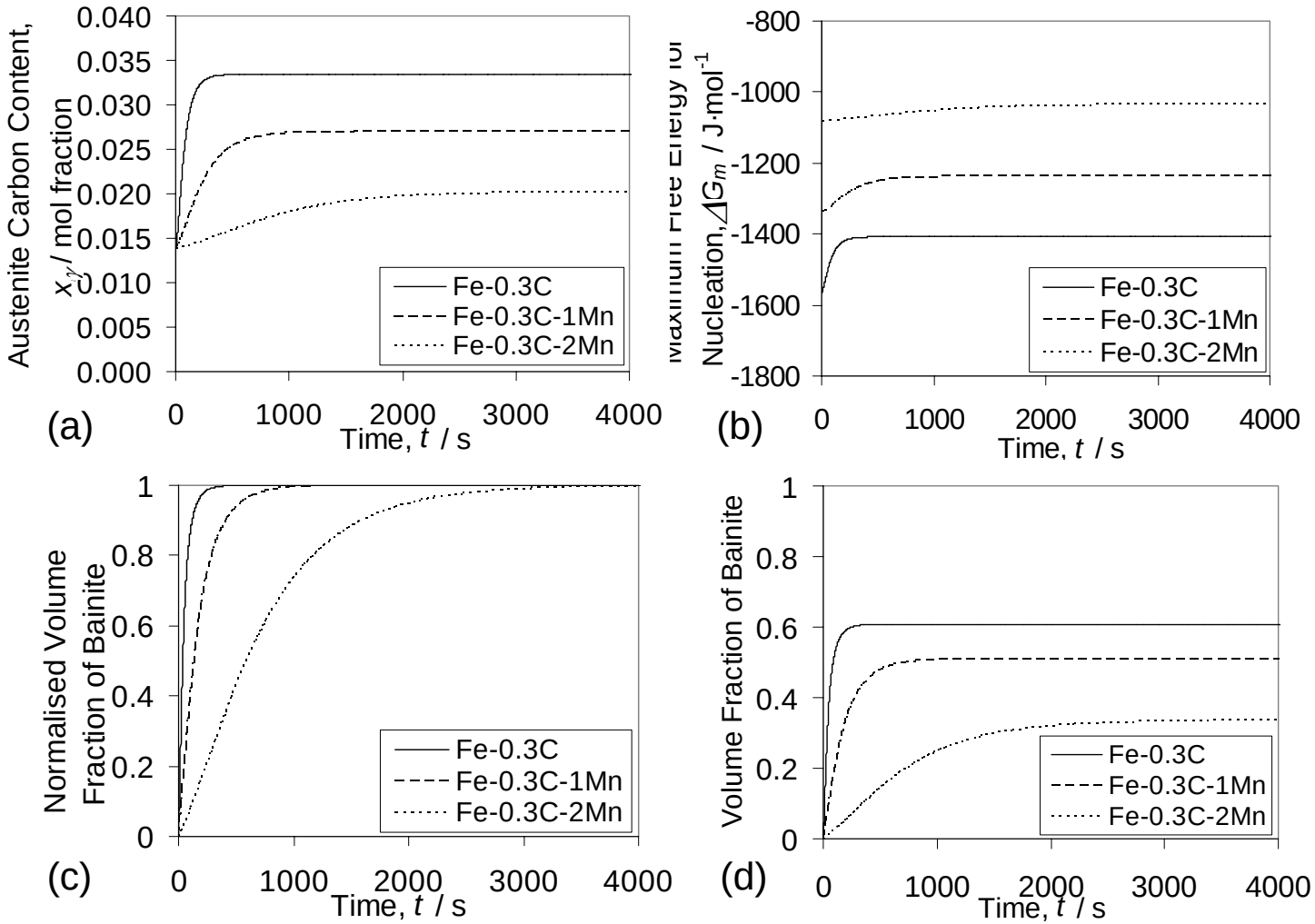
Austenite Carbon Content, x_γ / mol fraction
0.040
0.035
0.030
0.025
0.020
0.015
0.010
0.005
0.000
0
1000
2000
3000
4000
Time, t / s
Fe-0.3C
Fe-0.3C-1Mn
Fe-0.3C-2Mn
(a)
Maximum Free Energy for Nucleation, ΔG_m / J·mol^{-1}
-800
-1000
-1200
-1400
-1600
-1800
(b)
Normalised Volume Fraction of Bainite
1
0.8
0.6
0.4
0.2
0
(c)
Volume Fraction of Bainite
(d)

Figure 3

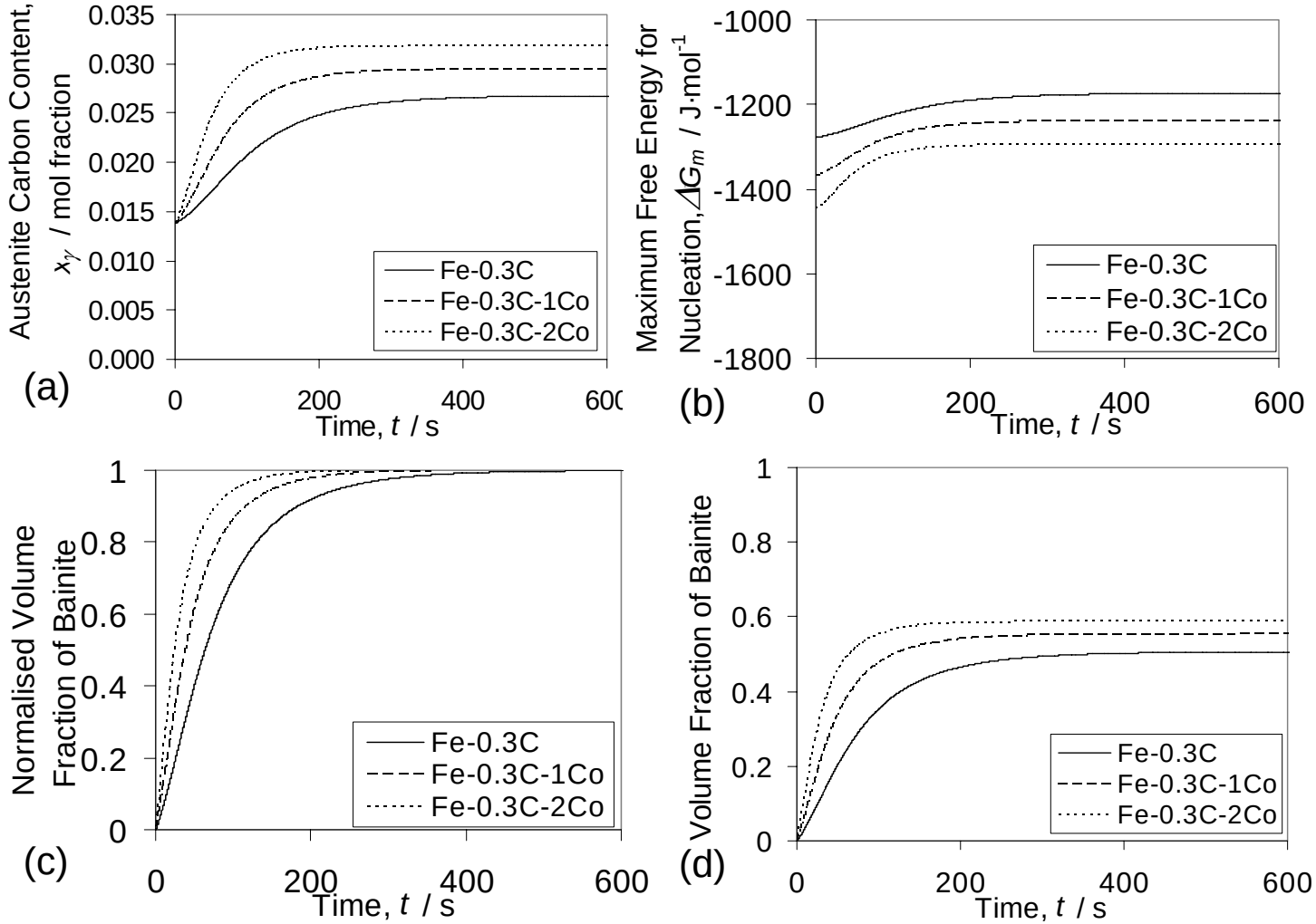
Austenite Carbon Content, x_γ / mol fraction
0.035
0.030
0.025
0.020
0.015
0.010
0.005
0.000
0
200
400
600
Time, t / s
Fe-0.3C
Fe-0.3C-1Co
Fe-0.3C-2Co
(a)
Maximum Free Energy for Nucleation, ΔG_m / J·mol^{-1}
-1000
-1200
-1400
-1600
-1800
0
200
400
600
Time, t / s
Fe-0.3C
Fe-0.3C-1Co
Fe-0.3C-2Co
(b)
Normalised Volume Fraction of Bainite
1
0.8
0.6
0.4
0.2
0
0
200
400
600
Time, t / s
Fe-0.3C
Fe-0.3C-1Co
Fe-0.3C-2Co
(c)
Volume Fraction of Bainite
1
0.8
0.6
0.4
0.2
0
0
200
400
600
Time, t / s
Fe-0.3C
Fe-0.3C-1Co
Fe-0.3C-2Co
(d)

Figure 4